

## Fabrication and optical properties of lead silicate glass holey fibers

H. Ebendorff-Heidepriem\*, P. Petropoulos, R. Moore, K. Frampton, D.J. Richardson, T.M. Monro

*Optoelectronics Research Centre, University of Southampton, Southampton SO17 1BJ, U.K.*

\* *Corresponding author: tel: +44-23-8059-2825, fax: +44-23-8059-3149, e-mail: [heh@orc.soton.ac.uk](mailto:heh@orc.soton.ac.uk)*

### Abstract

We report on recent progress in lead silicate holey fibres for nonlinear device applications. Improvements in the fabrication have resulted in core diameters as small as 1.7  $\mu\text{m}$ , increased air-suspension of the core and reduced propagation loss of 2.6 dB/m. This small core fibre exhibits a record nonlinearity of  $640 \text{ W}^{-1} \text{ km}^{-1}$ .

**PACS:** 42.65.-k; 42.81Bm; 42.81.Dp; 81.05.Kf

**Keywords:** holey optical fibres, microstructured optical fibres, fibre fabrication, nonlinearity

### 1. Introduction

Since the first microstructured fibre was made in 1996 [1], holey fibres (HFs) have attracted growing attention. Compared with conventional fibre types, they offer the combination of wavelength-scale features and design flexibility, which leads to a significantly broader range of optical properties than conventional fibres [2]. In particular, small core holey fibres allow the realization of fibres with a high effective nonlinearity per unit length. Such fibres promise the development of compact nonlinear devices that can operate at low powers.

In these fibres, the large index contrast between glass and air and the small core dimensions provide tight mode confinement, which allows substantial increase of the effective fibre nonlinearity relative to conventional fibre types [3]. Pure silica HFs with 70 times higher effective nonlinearity than standard telecommunication fibres have been demonstrated [4]. The material nonlinearity of compound glass [5] can be more than one order of magnitude larger than that of silica [6]. The combination of highly nonlinear glass composition such as lead silicate and a small core/high numerical aperture HF geometry allows a further dramatic increase of the fibre nonlinearity. Recently, we reported the fabrication of the first single-mode non-silica HF. This fibre was made from SF57 Schott (lead silicate) glass, for which an effective nonlinearity 500 times larger than in standard silica fibres was demonstrated [7].

For many applications, the sign and magnitude of the fibre dispersion are as critical to device functionality and performance as the magnitude of the nonlinearity. In particular, anomalous dispersion is required to make use of soliton-effects whereas near-zero dispersion is crucial for supercontinuum generation [2]. Most nonlinear/high-index glasses have a high normal material dispersion at 1550 nm. Fortunately, the influence of the holey fibre geometry allows the material dispersion to be overcome. Using SF6 Schott glass (another lead silicate glass), Kumar et al. [8] showed that it is possible to achieve near-zero dispersion at 1550 nm. Recently, we demonstrated operation in the anomalous dispersion regime for a HF made from SF57 lead silicate glass [9], which has even larger normal material dispersion than SF6 at 1550 nm.

Silica HFs have typically been made by stacking capillaries to form the microstructured cladding region [2]. Glasses with low softening temperatures allow the use of extrusion as an alternative fabrication technology. Recently, this approach has been employed to produce structured HF preforms from lead silicate glasses [8,10].

In this paper, we report on the fabrication and properties of small core HFs made from SF57 lead silicate glass using extrusion to produce the structured fibre preform. Compared with previous fibres of this type [7], recent progress in the fabrication has resulted in improved structure, higher nonlinearity and lower loss, which make practical nonlinear devices more realistic.

## 2. Experimental procedures and results

### 2.1. Fabrication and fibre structure

The fibres were made from commercially available bulk SF57 Schott glass. The high lead concentration in this glass leads to a high refractive index of 1.8 at 1.53  $\mu\text{m}$  [11] and a nonlinear refractive index of  $4.1 \times 10^{-19} \text{ m}^2/\text{W}$  at 1.06  $\mu\text{m}$  [5]. SF57 glass has a low softening temperature of 520  $^{\circ}\text{C}$  [11], which allows the utilization of extrusion for glass processing.

The fibres were made in three steps. First, the structured preform (Fig. 1b) and jacket tube were produced using extrusion. Next, the structured preform, which had an outer diameter (OD) of about 16 mm, was reduced in scale on a fibre drawing tower to a cane of about 1.7 mm OD (Fig. 1c). In the last step, the cane was inserted within a jacket tube, and this assembly was drawn to the final fibre (Fig. 1d). Four different fibres were produced, and a summary of the fabrication conditions and properties of extruded preforms, canes and fibres are listed in Table 1.

In the extrusion process, a glass disk is heated up to a temperature near the softening point (520  $^{\circ}\text{C}$  for SF57), and then the glass is pressed through the die, whose exit structure determines the shape of the extruded glass samples as illustrated in Figs. 1a and b for a structured preform. The total extrusion time (including die filling and sample formation) is similar for the three preforms. However, the time to produce preform P3 was clearly shorter

(see Table 1). The quality of the extruded glass samples in terms of defects and bubbles was examined using optical microscopy. At the outer and inner surface of the preform walls, localized defects were found. Compared with P1 and P2, we observed that preform P3 contains fewer such defects at the inner wall surface. For further improvement of the surface quality, preform P3 was cleaned with methanol prior to the cane drawing process.

From each assembly (cane within jacket tube), we have drawn more than 200 meters of fibre with core diameters in the range 1.7-2.9  $\mu\text{m}$ . Fibres F2b and F3 were made from annealed canes and jacket tubes. Good drawing stability was achieved for these fibres, whereas fibres F1 and F2a (which were not annealed) broke several times during drawing.

The dimensions of the structural features within the HFs were measured using scanning electron microscopy (SEM). The four different HFs have very similar cross-sectional profiles. The core is optically isolated from the outer solid glass region by three fine supporting struts (Fig. 1d). The core diameter was adjusted during fibre drawing by appropriate choice of the external fibre OD. For cores of 1.7-2.3  $\mu\text{m}$  diameter, the struts are  $\approx 5 \mu\text{m}$  long and 250 nm thick (Fig. 1d). The variations in core diameter for a single fibre with constant OD ( $\pm 2\%$ ) are within the measurement error of 5%. The variations in strut length and thickness relative to the core size are about 20% between fibres and 10% or less in a single fibre. Note that the measurement error is estimated to be 5% for the strut length and 8% for the strut thickness.

## *2.2. Optical properties*

Propagation loss of the fibres was measured at 1550 nm using free space coupling from a laser diode and the cut-back method. Fibre F1 exhibits loss values ranging from 5 to 18 dB/m (Table 1). Fibres F2a and F2b demonstrate higher losses of 9-13 dB/m. Note that the difference of 4 dB/m in the average loss values of longer fibre samples (2-3m) is clearly

larger than the measurement error of  $\pm 1$  dB/m. Fibre F3 exhibits the smallest loss of 2.6 dB/m.

In fibre F1, which has a  $1.7 \mu\text{m}$  core, robust single-mode guidance was observed at 1550 nm. The mode profile of this fibre has been predicted using the SEM image of the fibre structure and a full-vectorial implementation of the orthogonal function method [12]. The predicted mode profile at 1550 nm is superimposed on the index profile in Fig. 2. The predicted effective mode area,  $A_{\text{eff}}$ , for the  $1.7 \mu\text{m}$  core is  $2.6 \mu\text{m}^2$ .

The measurement of the effective nonlinearity and mode area of the fibre F1 at 1550 nm was based on measurement of the nonlinear phase shift induced through self-phase modulation, with a dual frequency beat signal propagating through the fibre [13]. The nonlinear phase shift was measured using a sample of 0.37 m length. Given the measured loss of 9 dB/m at 1550 nm for this sample, this corresponds to an effective fibre length of 0.26 m. The nonlinear phase shift is plotted in Fig. 3 as a function of the input power. From the slope of the linear fit and taking into account the effective length of the test fibre, an average value of the effective nonlinear coefficient,  $\gamma$ , was estimated to be  $640 \pm 60 \text{ W}^{-1} \text{ km}^{-1}$ . Assuming the value of the nonlinear refractive index,  $n_2=4.1 \times 10^{19} \text{ m}^2/\text{W}$ , from Ref. [5], the effective mode area at  $\lambda = 1550 \text{ nm}$  was calculated via  $\gamma = 2\pi n_2 / (\lambda A_{\text{eff}})$  [6] to be  $A_{\text{eff}} \approx 2.6 \pm 0.3 \mu\text{m}^2$ , in excellent agreement with the prediction (see above and Fig. 2).

### 3. Discussion

The four different HFs produced are almost identical in structure; they vary only slightly in the strut length and thickness relative to the core size, which can be adjusted by adjusting the fibre OD during the drawing process. This demonstrates the excellent reproducibility possible using this technique.

The fibres presented here have an improved structure compared with previous fibres of this type [7]. Full collapse of the canes onto the jacket tubes has been achieved without decreasing the size of the air holes and struts relative to the cores. The struts of the fibres presented here are more than two times longer and almost two times thinner, which ensures that the core is optically isolated from the external environment, and thus that confinement loss has been reduced to negligible levels [14]. In addition, the core dimensions have been reduced to increase mode confinement.

Good stability of fibre drawing has been achieved by annealing of canes and jacket tubes. The fast cooling rate during cane drawing and extrusion results in stresses in the glass, which are removed by annealing. We believe that the drawing instability of the two fibres F1 and F2a made from non-annealed jackets/canes is due to stress within the canes and/or extruded tubes.

The low loss of 2.6 dB/m for fibre F3 is to our knowledge the lowest value reported for a compound glass holey fibre. The large variations of loss values in fibre F1 indicate localized losses, possibly due to defects in the preform. In contrast, fibre F3 exhibits consistent loss values over several tens of meters.

The temperature, total extrusion time and fabrication conditions of the canes and fibres were similar for each of the four fibres produced. Therefore, thermally induced effects, such as phase separation within the glass or incorporation of water from the ambient atmosphere into the glass cannot account for the substantially lower loss of fibre F3. In small core HFs, the principal cause of loss is typically introduced by surface roughness at the core/air interface [15]. Thus, the substantially lower loss of fibre F3 is likely to be due to improved surface quality inside the corresponding preform P3. Indeed, in contrast to P1 and P2, preform P3 was cleaned, and it exhibits fewer defects at the inner surface of the preform wall. The latter result correlates with the faster extrusion of the actual preform. Further examination is needed to

understand the impact of the extrusion rate on the surface finish of the extruded preform. In addition, the lack of localised losses in fibre F3 supports the supposition that surface imperfections have been reduced. Hence we suggest that the reduced surface defects and/or the cleaning of the preform are responsible for the improved air/glass interfaces (and thus lower loss) in fibre F3. Further investigations are required to find out which effect is dominant.

#### **4. Summary and Conclusions**

Holey fibres with cores as small as  $1.7 \mu\text{m}$  have been produced from SF57 lead-silicate glass using extrusion technique for preform fabrication. Low propagation loss of  $2.6 \text{ dB/m}$  has been achieved as a result of improvements in the fabrication procedures for these fibres.

The tight mode confinement achieved by the improved fibre structure together with the high nonlinear refractive index of the lead silicate glass has resulted in a very high effective nonlinearity of  $640 \text{ W}^{-1} \text{ km}^{-1}$ . This is to our knowledge the highest nonlinearity reported for an optical fibre. It is more than 600 times larger than that of standard telecommunications fibres. First Raman soliton experiments with the fibres confirmed the high nonlinearity and revealed anomalous dispersion [9].

The extremely high nonlinearity, anomalous dispersion and low loss at  $1550 \text{ nm}$  highlight the enormous potential of the lead silicate holey fibres for optical processing applications. We expect that yet further improvements in the fabrication leads to losses near the value of the bulk glass ( $\sim 0.3 \text{ dB/m}$  [11]), which makes practical nonlinear devices possible.

## References

- [1] J.C. Knight, T.A. Birks, P.St.J. Russell, D.M. Atkin, *Opt. Lett.* 21 (1996) 1547.
- [2] T.M. Monro, D.J. Richardson, *C. R. Physique* 4 (2003) 175.
- [3] N.G.R. Broderick, T.M. Monro, P.J. Bennett, D.J. Richardson, *Opt. Lett.* 24 (1999) 1395.
- [4] J.H. Lee, W. Belardi, K. Furusawa, P. Petropoulos, Z. Yusoff, T.M. Monro, D.J. Richardson, *IEEE Photon. Technol. Lett.* 15 (2003) 440.
- [5] S.R. Friberg, P.W. Smith, *IEEE J. Quant. Electron.* 23 (1987) 2089.
- [6] G.P. Agrawal, *Nonlinear fibre Optics*, Academic Press, San Diego 1995
- [7] T.M. Monro, K. M. Kiang, J.H. Lee, K. Frampton, Z. Yusoff, R. Moore, J. Trucknott, D.W. Hewak, H.N. Rutt, D.J. Richardson, *Proc. Optical Fibre Communication Conference OFC 2002*, postdeadline paper FA1
- [8] V.V. Ravi Kanth Kumar, A.K. George, W.H. Reeves, J.C. Knight, P.St.J. Russell, *Opt. Express* 10 (2002) 1520.
- [9] P. Petropoulos, T.M. Monro, H. Ebendorff-Heidepriem, K. Frampton, R.C. Moore, H.N. Rutt, D.J. Richardson, *Proc. Optical Fibre Communication Conference OFC 2003*, postdeadline paper FA1
- [10] K. M. Kiang, K. Frampton, T.M. Monro, R. Moore, J. Trucknott, D.W. Hewak, D.J. Richardson, H.N. Rutt, *Electron. Lett.* 38 (2002) 546.
- [11] *Schott Optical Glass Catalogue*
- [12] T.M. Monro, D.J. Richardson, N.G.R. Broderick, P.J. Bennett, *J. Lightwave Technol.* 17 (1999) 1093.



- [13] A. Boskovich, S.V. Chernikov, J.R. Taylor, L. Gruner-Nielsen, O.A. Levring, *Opt. Lett.* 21 (1996) 1966.
- [14] L. Poladian, N.A. Issa, T.M. Monro, *Opt. Express* 10 (2002) 449.
- [15] K. Tajima, J. Zhou, K. Nakajima, K. Sato, *Proc. Optical Fibre Communication Conference OFC 2003*, postdeadline paper PD1-1

## **Table captions**

- 1: Fabrication conditions and properties of extruded preforms, canes and fibres. For details see text.

## **Figure captions**

- 1: (a) cross section of a die used for extruding a structured preform, (b) extruded preform P2, (c) SEM image of the cane C2, (d) SEM image of the fibre F2a.
- 2: Core structure with predicted mode profile for fibre F1.
- 3: Measured nonlinear phase shift as a function of input power to the fibre F1. The line designates linear regression fit.

Table 1: Fabrication conditions and properties of extruded preforms, canes and fibres. For details see text.

preform	extrusion time		cane	fibre	annealing of cane and tube	drawing stability	core diameter ( $\mu\text{m}$ )	fibre loss (dB/m)
	total (min)	sample (min)						
P1	$145 \pm 5$	$115 \pm 5$	C1	F1	no	fibre broke	$1.7 \pm 0.1$	$5 \dots 18 \pm 1$
P2	$130 \pm 5$	$125 \pm 5$	C2	F2a	no	fibre broke	$1.7 \pm 0.1$	$9 \dots 13 \pm 1$
				F2b	yes	good	$2.3 \pm 0.1$	$10 \pm 1$
P3	$120 \pm 5$	$70 \pm 5$	C3	F3	yes	good	$2.0 \pm 0.1$	$2.6 \pm 0.5$

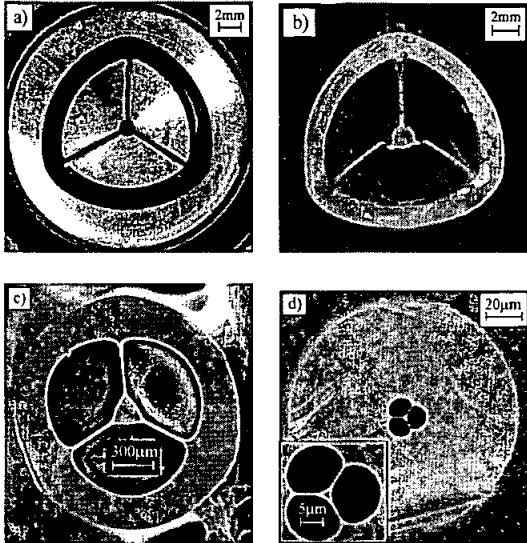


Figure 1: (a) cross section of a die used for extruding a structured preform, (b) extruded preform P2, (c) SEM image of the cane C2, (d) SEM image of the fibre F2a.

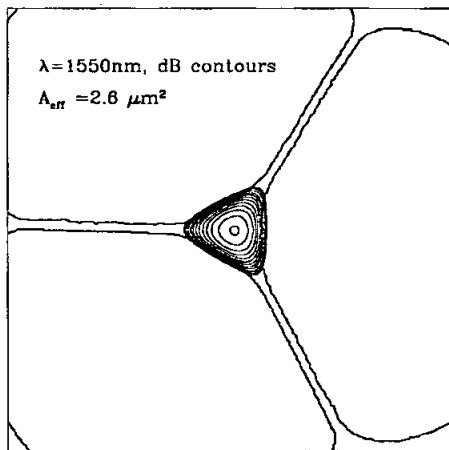


Figure 2: Core structure with predicted mode profile for fibre F1.

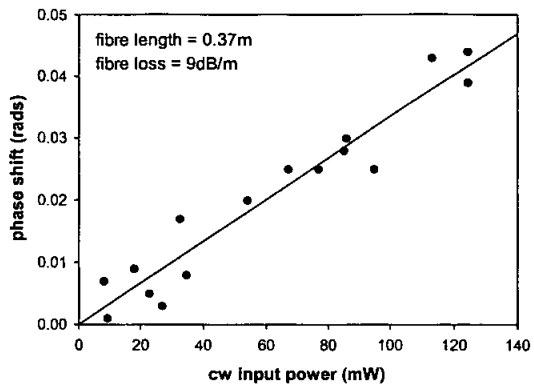


Figure 3: Measured nonlinear phase shift as a function of input power to the fibre F1. The line designates linear regression fit.